Turkish Journal of Chemistry

Volume 47 | Number 5 Article 22

10-31-2023

Comparatively sonophotochemical and photochemical studies of phthalocyanines with cationic substituents on nonperipheral positions

MUKADDES ÖZÇEŞMECİ

CEREN CAN KARANLIK

ALİ ERDOĞMUŞ

ESİN HAMURYUDAN

Follow this and additional works at: https://journals.tubitak.gov.tr/chem

 Part of the Chemistry Commons

Recommended Citation

ÖZÇEŞMECİ, MUKADDES; KARANLIK, CEREN CAN; ERDOĞMUŞ, ALİ; and HAMURYUDAN, ESİN (2023) "Comparatively sonophotochemical and photochemical studies of phthalocyanines with cationic substituents on nonperipheral positions," *Turkish Journal of Chemistry*: Vol. 47: No. 5, Article 22. https://doi.org/10.55730/1300-0527.3602
Available at: https://journals.tubitak.gov.tr/chem/vol47/iss5/22

This Article is brought to you for free and open access by TÜBİTAK Academic Journals. It has been accepted for inclusion in Turkish Journal of Chemistry by an authorized editor of TÜBİTAK Academic Journals. For more information, please contact academic.publications@tubitak.gov.tr.

TÜBİTAK

Turkish Journal of Chemistry

http://journals.tubitak.gov.tr/chem/

Research Article

Turk J Chem
(2023) 47: 1160-1168
© TÜBİTAK
doi:10.55730/1300-0527.3602

Comparatively sonophotochemical and photochemical studies of phthalocyanines with cationic substituents on nonperipheral positions

Mukaddes ÖZÇEŞMECİ[1], Ceren CAN KARANLIK[2], Ali ERDOĞMUŞ[2], Esin HAMURYUDAN[1,*]
[1]Department of Chemistry, Faculty of Science and Letters, Istanbul Technical University, İstanbul, Turkiye
[2]Department of Chemistry, Faculty of Science and Letters, Yıldız Technical University, İstanbul, Turkiye

Received: 16.04.2023 • **Accepted/Published Online:** 26.09.2023 • **Final Version:** 31.10.2023

Abstract: The term sonophotodynamic therapy (SPDT) refers to a combination of sonodynamic therapy (SDT) and photodynamic therapy (PDT), in which the efficacy of the treatment is boosted by utilizing the proper amount of a sensitizer that is responsive to both light and ultrasound. Although it has been proven in photophysicochemical studies that SPDT enhances singlet oxygen production, related studies in the literature are very limited. Considering this situation, this study aims to investigate the efficacy of synthesized phthalocyanines in terms of PDT and SPDT. The singlet oxygen quantum values calculated as 0.13 for **5**, 0.44 for **6**, and 0.61 for **7** in photochemical (PDT) application increased to 0.18, 0.86, and 0.92, respectively, with sonophotochemical (SPDT) application. According to the results, singlet oxygen production was more efficient with SPDT. This work will add to the body of knowledge on employing the SPDT approach to increase singlet oxygen generation.

Key words: Photodynamic therapy, phthalocyanine, singlet oxygen, sonophotodynamic therapy.

1. Introduction

Cancer is one of the diseases that negatively affect human health worldwide [1,2]. Great success has been achieved with traditional clinical treatments of cancer, such as surgical treatment, chemotherapy, and radiotherapy, and these are still being applied [3,4]. However, these treatment methods have many disadvantages as long-term side effects, toxicity, drug resistance, and low selectivity. For this reason, improving new treatment methods that reduce the death rate and increase the patient's quality of life in the fight against cancer is very important [3,5].

A potential therapy called photodynamic therapy (PDT) combines three elements: light, a medication called a photosensitizer, and molecular oxygen that damages tumor cells by photodamage [6-10]. Although this approach has several benefits, its effectiveness in treating deeply positioned cancers has been constrained by low light penetration into tissue layers [5,11]. Recently, a new and promising method, known as sonodynamic therapy (SDT), derived from PDT has emerged [12-15]. The main difference between the two methods is activating the sensitizers. In SDT, the sensitizer is activated by ultrasound rather than by light [16,17]. However, this method requires high concentrations of sensitizers, which can result in toxicity [5,18]. In order to overcome all these problems, a new approach called sonophotodynamic therapy (SPDT) is derived by combining PDT and SDT methods [19-23]. The sensitizers selected in SPDT are nontoxic structures with high sonophotosensitivity, they have stable chemical composition, low aggregation tendency, and good solubility properties [5,16,24].

Phthalocyanines (Pcs) are aromatic macrocycles that have undergone substantial research due to their distinctive characteristics and wide range of uses in biology, medicine, and materials [25-38]. Pcs are among the promising second- and third-generation photosensitizers due to their high absorption in the phototherapeutic window and their efficiency in reactive oxygen generation. Also, diamagnetic central metal ions (such as Zn^{2+}, In^{3+}, and Ga^{3+}) containing Pcs are used as photosensitizers due to their efficiency in reactive oxygen generation and high singlet oxygen quantum yields.

The low solubility and high aggregation of Pcs in common organic solvents are a disadvantage for many applications. Especially water solubility is important in biological and medical applications [39]. As a result, it is necessary to construct Pcs with ionic or nonionic substituents in peripheral, nonperipheral, or axial places. Cationic Pcs are obtained with quaternization of aliphatic or aromatic nitrogen atoms in the molecule [27,30,31,40-42]. We have quaternized 1,3-bis-

* Correspondence: esin@itu.edu.tr

This work is licensed under a Creative Commons Attribution 4.0 International License.

(trimethylamino)-2-propoxy groups where Pcs are substituted with methyl iodide, leading to their water-soluble derivatives. So an important result, namely water solubility, has been provided. Comparatively to metal-free Pc, the photophysical, photochemical, and sonophotochemical characteristics of the produced metallo-Pc derivatives (M: Zn(II) and In(III)Cl) were examined.

2. Results and discussion

2.1. Synthesis and characterization

The synthetic processes for producing the metal-free Pc and metallo-Pc derivatives (**2**-**7**) are shown in Figure 1. Compound **1** was prepared according to the reported procedure [43]. Compound 1 and lithium metal were combined in n-pentanol for the production of the metal-free Pc derivative (**2**), which was subsequently acidified with 1 mL of glacial acetic acid. The indium(III) Pc derivative (**4**) was synthesized by the addition of $InCl_3$ to compound **2** in 2-dimethylaminoethanol. UV-Vis spectra obtained in 2-dimethylaminoethanol showed the elimination of the Q band of metal-free Pc and the emergence of a new Q band of indium Pc. Water soluble cationic Pcs **5** and **7** were obtained with quaternization of aliphatic nitrogen atoms in compounds **2** and **4** with methyl iodine. Pcs **3** and **6** were prepared using the synthetic procedure described in Ref. [27].

In this study, all synthesized compounds were characterized using several spectroscopic methods. Each compound's spectral information matched the formulations.

The FT-IR spectra of **2** and **4** showed no strong nitrile vibrations at 2229 cm^{-1}, which supported the production of Pc derivatives. Synthesized Pcs' FT-IR spectra were similar, except for the metal-free derivatives (**2** and **5**). They displayed additional absorption bands attributed to the -NH stretching vibrations at 3291 cm^{-1}. Broad peaks were observed in the ^{1}H NMR spectra in DMSO-d_6 due to the mixed structural isomers of tetrasubstituted Pcs. The multiplets of aromatic protons of Pcs were seen at 8.28–7.40 (**2**), 9.22–7.78 (**4**), 9.11–7.49 (**5**), and 9.41–8.17 (**7**) ppm, respectively. The OCH protons were observed as multiplets at 5.30 (**2**), 5.12 (**4**), 6.27 (**5**), and 6.16 (**7**) ppm, respectively. The NCH_2 protons were observed at 3.81 (**2**), 2.83 (**4**), 4.63 (**5**), and 4.19 (**7**) ppm, respectively. Also, $-NCH_3$ protons were seen at 3.11 (**2**), 2.42 (**4**), 3.09 (**5**), and 3.43 (**7**) ppm, respectively. The inner core protons were also monitored with broad chemical shifts at –1.38 (for **2**) and –1.40 (for **5**) ppm.

The molecular peaks at m/z 1091.192 $[M]^+$ (for **2**), 1239.159 $[M]^+$ (for **4**), 1338.573 $[M - 7I]^+$, 1211.111 $[M - 8I]^+$ (for **5**), 1740.699 $[M - 5I]^+$, 1360.171 $[M - 8I]^+$ (for **7**) were seen in the MALDI-TOF mass spectra.

Two prominent peaks can be seen in the electronic absorption spectra of Pcs **2** and **4** in THF: the typical ligand-centered π–π* transitions of a monomeric metal-free (**2**) and indium(III) (**4**) Pcs with Q-band maxima at 694 and 726 (for **2**) and 717 (for **4**) nm. Due to its D_{2h} symmetry, the Q band of the metal-free derivative (**2**) showed signs of splitting [44]. The additional Pcs-specific bands, or B bands, were seen at 319 and 322 nm for Pcs **2** and **4**, respectively. Indium(III) phthalocyanine (**4**) possesses Q bands that change bathochromically at 17 nm when compared to the λ_{max} value of the

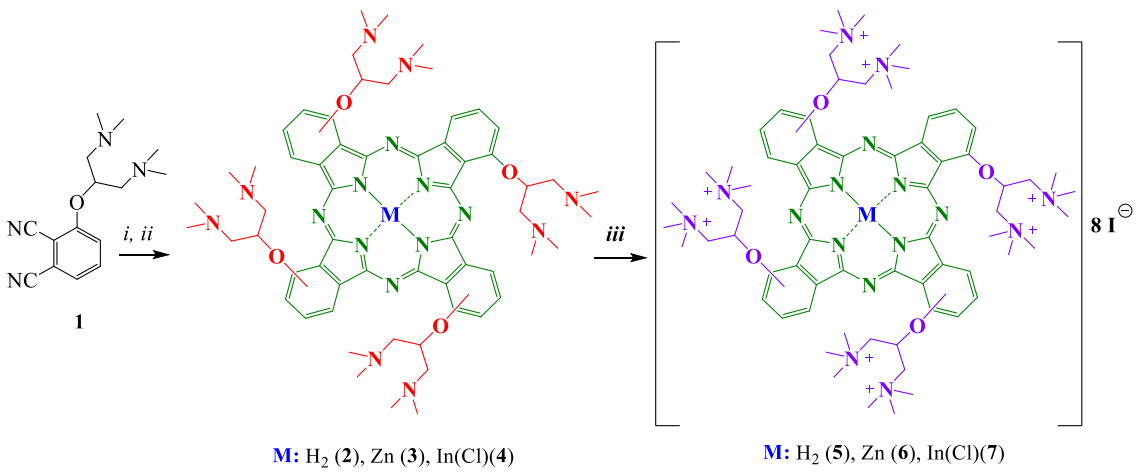


Figure 1. Synthesis of phthalocyanines (**2**-**7**) (*i*: lithium metal, *n*-pentanol, 145 °C, acetic acid; *ii*: metal salt, 2-dimethylaminoethanol, 140 °C, 24 h, *iii:* CH_3I, $CHCl_3$, at dark, reflux temperature).

zinc(II) phthalocyanine (**3**) [27]. This can be explained by the fact that indium, as the central metal ion, remains outside the cavity due to its larger radius. Quaternized derivatives of compounds **5** and **7** showed B bands in DMSO at 322 and 335 nm, respectively. In DMSO, the Q bands were recorded at 693 (for **5**) and 720 nm (for **7**). In addition, the absorption spectra of quaternized Pcs **5** and **7** in water displayed B bands at 319 (for **5**) and 335 (for **7**) nm and Q bands at 693 (for **5**) and 715 (for **7**) nm (Figure 2).

2.2. Photophysical and photochemical studies

2.2.1. Fluorescence quantum yield (Φ_F)

Fluorescence characteristics of molecules enable traceability of their in biological systems in PDT applications. Here, the fluorescence characteristics of **5**, **6**, and **7** were examined in DMSO, and they displayed emission bands at 705 nm with fluorescence quantum yield (Φ_F) of 0.05 (for **5**), at 717 nm with Φ_F of 0.056 (for **6**) and 727 nm with Φ_F of 0.030 (for **7**). The results were recorded in Table, and Figure 3 depicts the obtained spectral changes (absorption, emission, and excitation).

In DMSO, unsubstituted ZnPc has a greater fluorescence quantum yield (Φ_F: 0.20) [45] than Pcs (**5**-**7**). The presence of heavy atoms such as indium in the central cavity of Pcs contributes to ISC, resulting in high singlet oxygen quantum yield and low fluorescence quantum yield. The fluorescence quantum yield of unsubstituted indium(III) Pc (ClInPc) was calculated as 0.018 [46] in DMSO. A slight increase in Φ_F value of compound **7** was observed compared to ClInPc.

2.2.2. Singlet oxygen quantum yields (Φ_Δ)

When excited with a specific wavelength of light or ultrasound frequency, sensitizers can change molecular oxygen into reactive oxygen species. Singlet oxygen, one of these reactive oxygen species, constitutes one of the fundamental components of PDT. Although the sensitizer directly influences the formation of singlet oxygen, the sensitizer's stimulation technique has a significant impact as well. In the stimulation of sensitizers, suitable wavelengths of light, ultrasound, and light/ultrasound can be used together. We describe it as "photodynamic therapy" when light is used as a stimulation method, "sonodynamic therapy" when sound waves are used, and "sonophotodynamic therapy" when ultrasound and light are used together [24]. Studies in the literature have shown that the SPDT approach increases singlet oxygen generation [13,17,45,47,48]. Using photodynamic and sonophotodynamic techniques, we investigated the relationship between

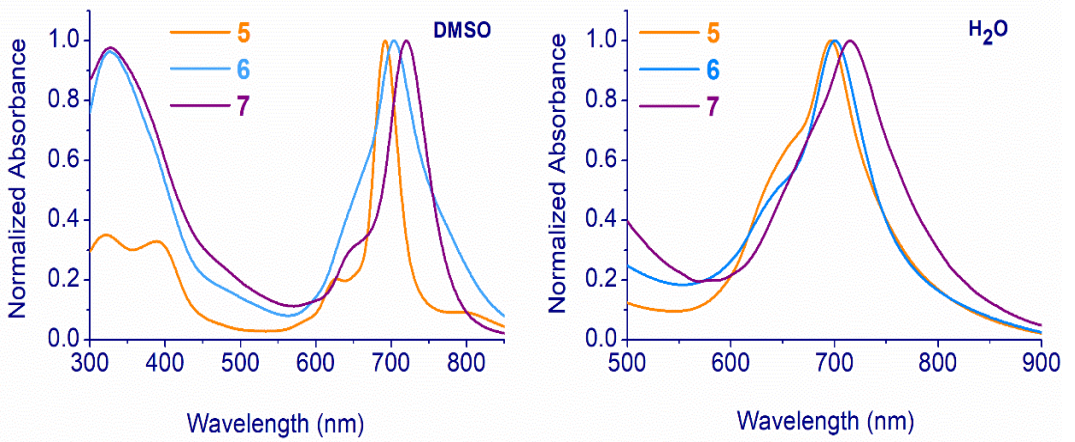


Figure 2. UV-Vis absorption spectra of **5**-**7** in DMSO (**a**) and water (**b**) at 1×10^{-5} M.

Table. Photophysicochemical properties of complexes (**5**-**6**) in DMSO.

Pcs	λ_{Abs} (nm)	λ_{Em} (nm)	Δ_{Stokes} (nm)	Log ε	Φ_F	Φ_d (10^{-4})	$\Phi_{\Delta(PDT)}$	$\Phi_{\Delta(SPDT)}$
5	693	704	11	4.55	0.05	8.7	0.13*	0.18
6	699	717	18	4.69	0.056	1.2	0.44*	0.86
7	720	727	7	4.47	0.030	1.4	0.61*	0.92

- Unsubstituted ZnPc (F_D): 0.67 in DMSO* was used as a standard in the singlet oxygen quantum yield measurements.

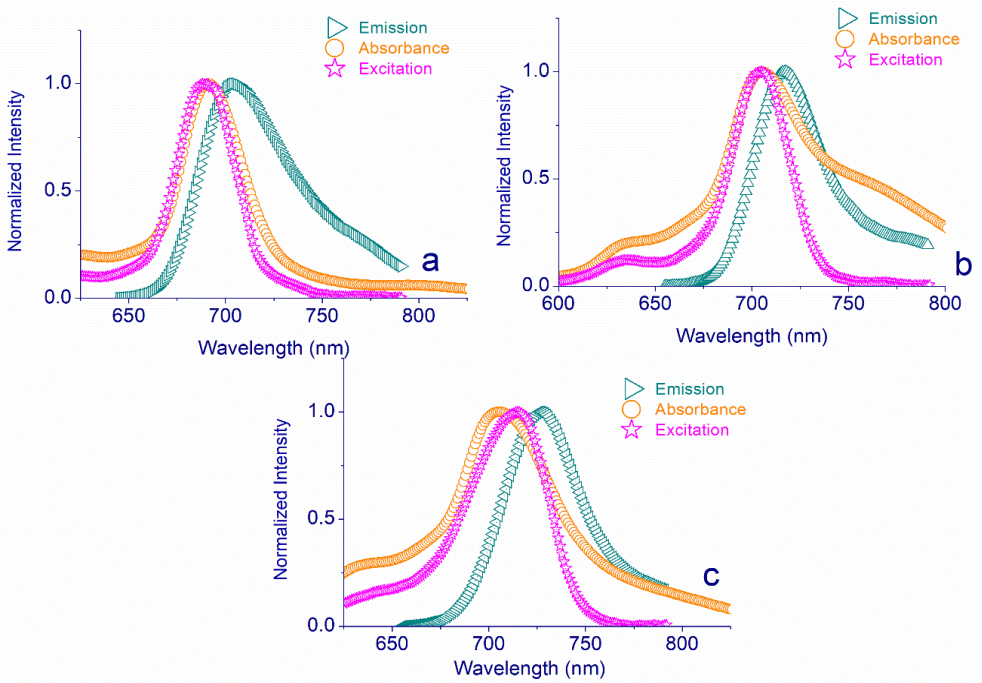


Figure 3. a) Absorption (693 nm), excitation (693 nm), and emission (704 nm) spectra of **5**, **b)** absorption (699 nm), excitation (699 nm), and emission (717 nm) spectra of **6**, **c)** absorption (720 nm), excitation (722 nm), and emission (727 nm) spectra of **7**.

singlet oxygen generation and irradiation method to evaluate the singlet oxygen-producing capacities of the cationic Pcs (**5**-**7**). The singlet oxygen quantum yields of cationic Pcs (**5**-**7**) were calculated for both methods using unsubstituted ZnPc as standard and 1,3-diphenylisobenzofuran (DPBF) as a chemical singlet oxygen quencher [49]. Pcs (**5**-**7**), standard ZnPc, and DPBF solutions were dissolved in DMSO and kept in a dim environment. In PDT and SPDT applications, the importance of water solubility stands out. However, most Pcs are insoluble or have serious aggregation behavior in water. Because of this, DMSO, a nontoxic solvent for biological cell investigations at the necessary concentration for PDT/SPDT application, has been chosen in related photophysical and photochemical studies [50,51].

In the measurements performed using the photochemical method, the solutions containing Pcs (**5**-**7**) and DPBF were exposed to light (intensity of 7.05×10^{15} photons s^{-1} cm^{-2}) every 5 s and the change in absorbance of DPBF at 417 nm was followed by using UV-Vis spectrophotometer. Table contains the singlet oxygen quantum yields of compounds **5**-**7**. The corresponding spectra and plot of the DPBF absorption reduction with time are displayed in Figures 4–6. The singlet oxygen quantum yields were calculated as 0.13 for **5**, 0.44 for **6**, and 0.61 for **7**. The results demonstrate that all cationic Pcs (**5**-**7**) promote the intersystem crossing (ISC) more strongly than unsubstituted ZnPc, boosting singlet oxygen generation while lowering fluorescence efficiency. The metal atom in the center is important for increasing the efficiency of the Pc molecule as a sensitizer. A heavy central atom such as indium provides a high singlet oxygen yield because it contributes to ISC. Therefore, indium Pcs can have high singlet oxygen quantum yields [52,53].

In studies carried out with the photosonochemical method, the solutions were first exposed to light for 5 s and to ultrasound (35 kHz) every 5 s, and a UV-Vis spectrophotometer was used to monitor the change in DPBF's absorbance at 417 nm. The SPDT approach yielded singlet oxygen quantum efficiencies of 0.18 for **5**, 0.86 for **6**, and 0.92 for **7**. It was observed that SPDT application increased the singlet oxygen formation considerably compared to PDT only. The mechanism of activating the sensitizer by the SDT method is not yet fully understood, but possible processes have been described [54]. In a study in which only light, only sound and light + sound were used together [55], the use of light + sound increased the singlet oxygen generating capacity more than the methods in which only light and only sound were used. Also, it has been observed that the method in which only light is used as a stimulant is more effective than the method in which only sound is used as a stimulant. In our different studies, we examined the effect of the stimulant on singlet oxygen production as photochemically and sonophotochemically and observed that singlet oxygen production increased significantly when light and ultrasound were used together [56,57]. It has also been

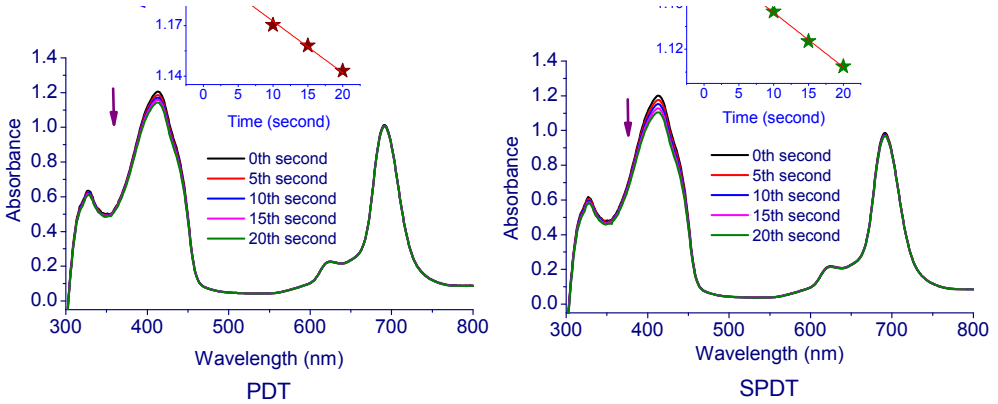


Figure 4. Representative absorption spectral changes during the determination of the singlet oxygen quantum yield of **5**.

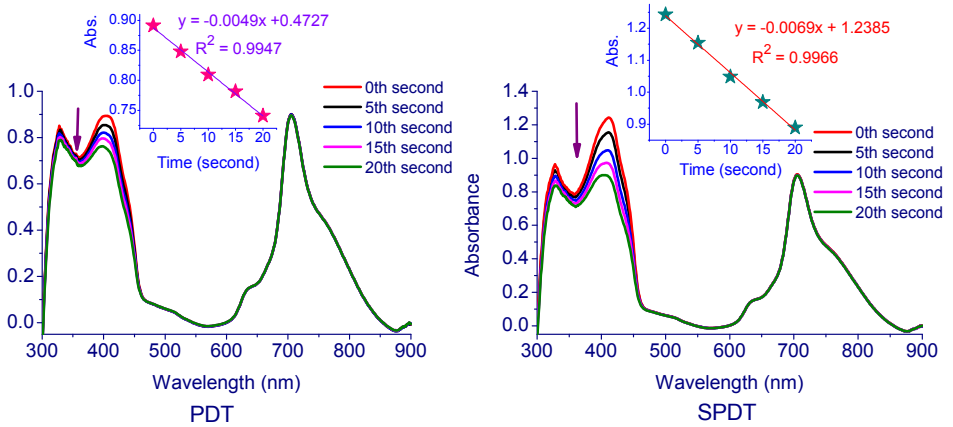


Figure 5. Representative absorption spectral changes during the determination of the singlet oxygen quantum yield of **6**.

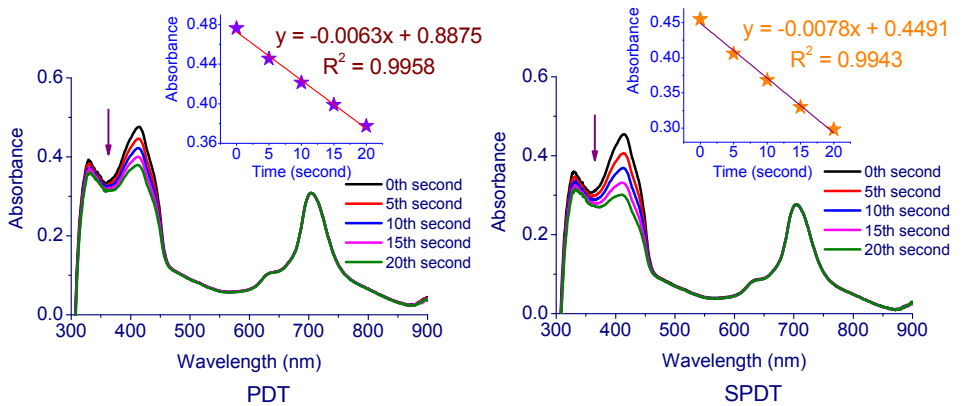


Figure 6. Representative absorption spectral changes during the determination of the singlet oxygen quantum yield of **7**.

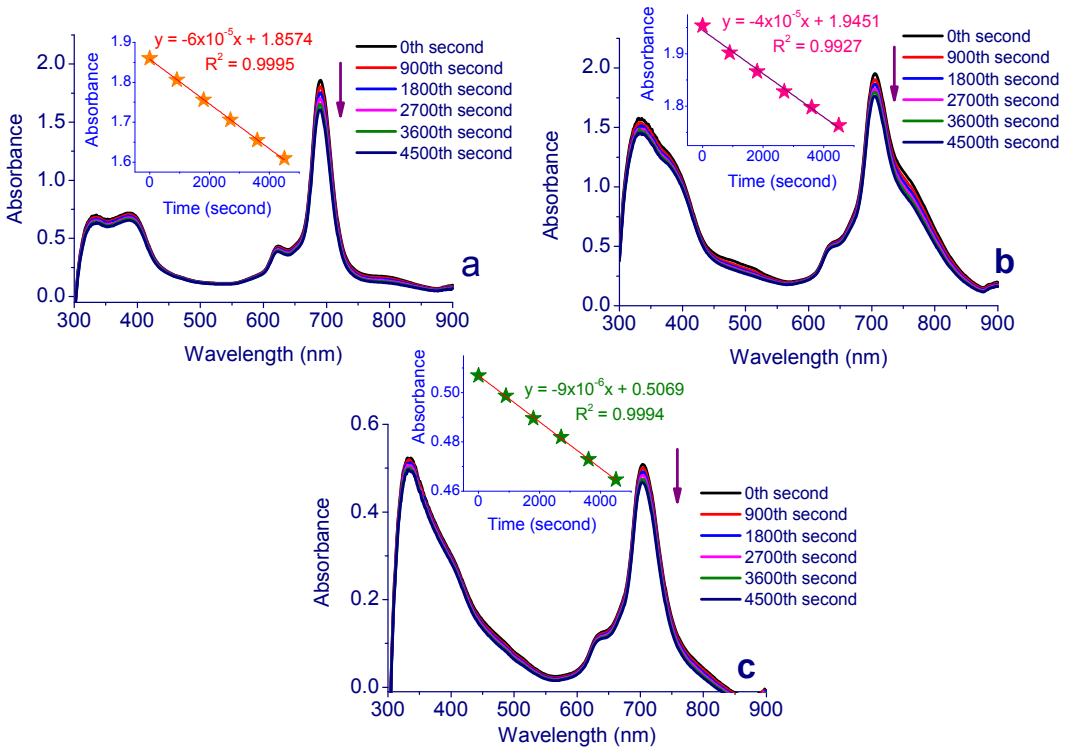


Figure 7. Representative absorption spectral changes during the determination of the photodegradation quantum yield of Pcs **a)** for **5**, **b)** for **6**, and **c)** for **7**.

reported that the ultrasound effect contributes to the formation of reactive oxygen species such as singlet oxygen. In this way, it was also stated that SPDT technique causes more deaths on various cancer cells than PDT [4, 58, 55].

2.2.3. Photodegradation quantum yields (Φ_d)

High singlet oxygen production, fluorescence, solubility in water or biocompatible solvents to accumulate in tumor tissue and photostability are expected properties of sensitizers for PDT and SPDT applications. Singlet oxygen production starts with the stimulation of the sensitizer, so it is very important for the treatment to keep the concentration of the sensitizer constant during the treatment. For this reason, the photostabilities of Pcs (**5**-**7**) were calculated by utilizing the change in the absorption band by exposing them to 5 min of photoirradiation via UV-Vis spectroscopy in the biocompatible solvent DMSO. Table contains the related data, while Figure 7 shows the spectra. The result showed that Pcs were stable during photodegradation. F_d values of the Pcs are 8.7×10^{-4} for **5**, 1.2×10^{-4} for **6**, and 1.4×10^{-4} for **7**. Obtained results are compared with the literature, and the photostability of Pcs agrees with those of other studies [59].

3. Conclusion

In this study, metal-free and metallophthalocyanines having 1,3-bis-(trimethylamino)-2-propoxy groups at the nonperipheral positions were synthesized and characterized. In addition, the capability of the Pcs to generate singlet oxygen was studied photochemically and sonophotochemically. In photochemical measurements, the singlet oxygen values were 0.13 for **5**, 0.44 for **6**, and 0.61 for **7**. In sonophotochemical measurements, the singlet oxygen values increased to 0.18 for **5**, 0.86 for **6**, and 0.92 for **7**. Based on the singlet oxygen quantum values formed by the different irradiation methods of the Pcs and their photostability during these application methods, especially metallo derivatives can be considered to be good sensitizing agents in PDT and SPDT applications.

Supplementary information

The materials and equipment, experimental section, and methods used for the photophysical, photochemical, and sonochemical properties of compounds are described in the "Supplementary information" section below.

Acknowledgement

This work was supported by the Research Fund of the Istanbul Technical University.

References

[1] Siegel R, Ma J, Zou Z, Jemal A. Cancer statistics. CA: A Cancer Journal for Clinicians 2014; 64: 9-29. https://doi.org/10.3322/caac.21208

[2] Zheng Y, Ye J, Li Z, Chen H, Gao Y. Recent progress in sono-photodynamic cancer therapy: From developed new sensitizers to nanotechnology-based efficacy-enhancing strategies. Acta Pharmaceutica Sinica B 2021; 11 (8): 2197-2219. https://doi.org/10.1016/j.apsb.2020.12.016

[3] Dy GK, Adjei AA. Understanding, recognizing, and managing toxicities of targeted anticancer therapies. CA: A Cancer Journal for Clinicians 2013; 63: 249-279. https://doi.org/10.3322/caac.21184

[4] Güzel E, Atmaca GY, Kuznetsov AE, Turkkol A, Bilgin MD et al. Ultrasound versus light: Exploring photophysicochemical and sonochemical properties of phthalocyanine-based therapeutics, theoretical study, and in vitro evaluations. ACS Applied Bio Materials 2022; 5 (3): 1139-1150. https://doi.org/10.1021/acsabm.1c01199

[5] Chen H, Zhou X, Gao Y, Zheng B, Tang F et al. Recent progress in development of new sonosensitizers for sonodynamic cancer therapy. Drug Discovery Today 2014; 19 (4): 502-509. https://doi.org/10.1016/j.drudis.2014.01.010

[6] Akkoç B, Samsunlu T, Işık Ş, Özçeşmeci M, Atmaca GY et al. Pegylated metal-free and zinc (II) phthalocyanines: synthesis, photophysicochemical properties and in vitro photodynamic activities against head, neck and colon cancer cell lines. Dalton Transactions 2022; 51: 10136-10147. https://doi.org/10.1039/d2dt00704e

[7] Sharman WM, Allen CM, van Lier JE. Photodynamic therapeutics: basic principles and clinical applications. Drug Discovery Today 1999; 4: 507-517. https://doi.org/10.1016/S1359-6446(99)01412-9

[8] Felsher DW. Cancer revoked: oncogenes as therapeutic targets. Nature Reviews Cancer 2003; 3 (5): 375-379. https://doi.org/10.1038/nrc1070

[9] McEwan C, Nesbitt H, Nicholas D, Kavanagh ON, McKenna K et al. Comparing the efficacy of photodynamic and sonodynamic therapy in non-melanoma and melanoma skin cancer. Bioorganic & Medicinal Chemistry 2016; 24 (13): 3023-3028. https://doi.org/10.1016/j.bmc.2016.05.015

[10] Shen XM, Zheng BY, Huang XR, Wang L, Huang JD. First silicon (IV) phthalocyanine-nucleoside conjugates with high photodynamic activity. Dalton Transactions 2013; 42: 10398-10403. https://doi.org/10.1039/c3dt50910a

[11] Trendowski M. Using the promise of sonodynamic therapy in the clinical setting against disseminated cancers. Chemotherapy Research and Practice 2015; 2015: 316015. https://doi.org/10.1155/2015/316015

[12] Umemura SI, Yumita N, Nishigaki R, Umemura K. Mechanism of cell damage by ultrasound in combination with hematoporphyrin. Japanese Journal of Cancer Research 1990; 81 (9): 962-966. https://doi.org/10.1111/j.1349-7006.1990.tb02674.x

[13] Karanlık CC, Atmaca GY, Erdoğmuş A. Improved singlet oxygen yields of new palladium phthalocyanines using sonochemistry and comparisons with photochemistry. Polyhedron 2021; 206: 115351. https://doi.org/10.1016/j.poly.2021.115351

[14] Trendowski M. The promise of sonodynamic therapy. Cancer and Metastasis Reviews 2014; 33: 143-160. https://doi.org/10.1007/s10555-013-9461-5

[15] Bakhshizadeh M, Moshirian T, Esmaily H, Rajabi O, Nassirli H et al. Sonophotodynamic therapy mediated by liposomal zinc phthalocyanine in a colon carcinoma tumor model: Role of irradiating arrangement. Iranian Journal of Basic Medical Sciences 2017; 20 (10): 1088-1092. https://doi.org/10.22038/IJBMS.2017.9410

[16] Wang X, Zhang W, Xu Z, Luo Y, Mitchell D et al. Sonodynamic and photodynamic therapy in advanced breast carcinoma: A report of 3 cases. Integrative Cancer Therapies 2009; 8: 283-287. https://doi.org/10.1177/1534735409343693

[17] Atmaca GY, Karanlık CC, Erdoğmuş A. Measurement of improved singlet oxygen generations of indium chloride phthalocyanines by comparatively sono-photochemical and photochemical studies. Dyes and Pigments 2021; 194: 109630. https://doi.org/10.1016/j.dyepig.2021.109630

[18] Karaoğlan GK. Synthesis of a novel zinc phthalocyanine with peripherally coordinated Ru (II) complexes; sono-photochemical, photochemical and photophysical studies. Journal of Molecular Structure 2022; 1261: 132886. https://doi.org/10.1016/j.molstruc.2022.132886

[19] Jin ZH, Miyoshi N, Ishiguro K, Umemura S, Kawabata K et al. Combination effect of photodynamic and sonodynamic therapy on experimental skin squamous cell carcinoma in C3H/HeN mice. The Journal of Dermatology 2000; 27: 294-306. https://doi.org/10.1111/j.1346-8138.2000.tb02171.x

[20] Li Q, Liu Q, Wang P, Feng X. Wang H et al. The effects of Ce6-mediated sono-photodynamic therapy on cell migration, apoptosis and autophagy in mouse mammary 4T1 cell line. Ultrasonics 2014; 54: 981-989. https://doi.org/10.1016/j.ultras.2013.11.009

[21] Atmaca GY. Investigation of the differences between sono-photochemical and photochemical studies for singlet oxygen generation of indium phthalocyanine. Inorganica Chimica Acta 2021; 515: 120052. https://doi.org/10.1016/j.ica.2020.120052

[22] Kolarova H, Tomankova K, Bajgar R, Kolar P, Kubinek R. Photodynamic and sonodynamic treatment by phthalocyanine on cancer cell lines. Ultrasound in Medicine & Biology 2009; 35: 1397-1404. https://doi.org/10.1016/j.ultrasmedbio.2009.03.004

[23] Kessel D, Lo J, Jeffers R, Fowlkes JB, Cain C. Modes of photodynamic vs. sonodynamic cytotoxicity. Journal of Photochemistry and Photobiology B: Biology 1995; 28: 219-221. https://doi.org/10.1016/1011-1344(94)07111-z

[24] Atmaca GY, Aksel M, Keskin B, Bilgin MD, Erdoğmuş A. The photo-physicochemical properties and in vitro sonophotodynamic therapy activity of Di-axially substituted silicon phthalocyanines on PC3 prostate cancer cell line. Dyes Pigments 2021; 184: 108760. https://doi.org/10.1016/j.dyepig.2020.108760

[25] Leznoff CC, Lever ABP. Phthalocyanines: properties and applications. New York, VHC, 2004.

[26] Mckeown NB. Phthalocyanine materials: synthesis, structure and function. Press syndicate of the University of Cambridge, Cambridge. 1998.

[27] Özçeşmeci M, Sancar Baş S, Akkurt B, Bolkent Ş, Hamuryudan E. Synthesis, characterization and staining performance of peripherally and non-peripherally substituted metallo-phthalocyanines bearing 1,3-bis-(trimethylamino)-2-propoxy groups. New Journal of Chemistry 2020; 44: 7786-7794. https://doi.org/10.1039/d0nj01404d

[28] Demir F, Yenilmez HY, Koca A, Bayır ZA. Metallo-phthalocyanines containing thiazole moieties: Synthesis, characterization, electrochemical and spectroelectrochemical properties and sensor applications. Journal of Electroanalytical Chemistry 2019; 832: 254-265. https://doi.org/10.1016/j.jelechem.2018.11.003

[29] Ilgün C, Sevim AM, Çakar S, Özacar M, Gül A. Novel Co and Zn-Phthalocyanine dyes with octa-carboxylic acid substituents for DSSCs. Solar Energy 2021; 218: 169-179. https://doi.org/10.1016/j.solener.2021.02.042

[30] Nar I, Bortolussi S, Postuma I, Atsay A, Berksun E et al. A phthalocyanine-*ortho*-carborane conjugate for boron neutron capture therapy: Synthesis, physicochemical properties, and in vitro tests. ChemPlusChem 2019; 84: 345-351. https://doi.org/10.1002/cplu.201800560

[31] Özceşmeci M, Sancar-Baş S, Akkurt B, Hamuryudan E, Bolkent Ş. Synthesis and biological uses of A_3B type water-soluble phthalocyanine alternate to Alcian blue. ChemistrySelect 2018; 3 (45): 12805-12812. https://doi.org/10.1002/slct.201803371

[32] Dalkılıç Z, Cheong BL, Hyosung C, Nar I, Yavuz NK et al. Tetra and octa substituted Zn(II) and Cu(II) phthalocyanines: Synthesis, characterization and investigation as hole-transporting materials for inverted type-perovskite solar cells. Journal of Organometallic Chemistry 2020; 922: 121419. https://doi.org/10.1016/j.jorganchem.2020.121419

[33] Özçeşmeci M, Özçeşmeci İ, Sorar İ, Hamuryudan E. Thin films of fluorinated groups substituted metallophthalocyanines as an optical material. Inorganic Chemistry Communications 2017; 86: 209-212. https://doi.org/10.1016/j.inoche.2017.10.026

[34] Li B, Lin L, Lin H, Wilson BC. Photosensitized singlet oxygen generation and detection: Recent advances and future perspectives in cancer photodynamic therapy. Journal of Biophotonics 2016; 9 (11-12): 1314-1325. https://doi.org/10.1002/jbio.201600055

[35] Gümrükçü S, Özçeşmeci M, Sezer E, Ustamehmetoğlu B, Hamuryudan E. In-situ synthesis of phthalocyanines on electrospun TiO_2 nanofiber by solvothermal process for photocatalytic degradation of methylene blue. Turkish Journal of Chemistry 2021; 45 (6): 2034-2045. https://doi.org/10.3906/kim-2108-14

[36] Kobak RZU, Akyüz D, Koca A. Substituent effects to the electrochromic behaviors of electropolymerized metallophthalocyanine thin films. Journal of Solid State Electrochemistry 2016; 20 (5): 1311-1321. https://doi.org/10.1007/s10008-016-3120-z

[37] Özçeşmeci M, Özkan E, Hamuryudan E. Synthesis, characterization, and aggregation properties of functionalized polyfluorinated metallo-phthalocyanines. Journal of Porphyrins and Phthalocyanines 2013; 17: 972-979. https://doi.org/10.1142/S1088424613500764

[38] Kurt Ö, Özçeşmeci İ, Koca A, Gül A, Koçak MB. Synthesis, photophysical and electrochemical properties of novel hexadeca-substituted phthalocyanines bearing naphthoxy groups. Dyes and Pigments 2017; 137: 236-243. https://doi.org/10.1016/j.dyepig.2016.10.014

[39] Dumoulin F, Durmuş M, Ahsen V, Nyokong T. Synthetic pathways to water-soluble phthalocyanines and close analogs. Coordination Chemistry Reviews 2010; 254: 2792-2847. https://doi.org/10.1016/j.ccr.2010.05.002

[40] Moeini Alishah M, Yenilmez HY, Özçeşmeci İ, Sesalan BŞ, Altuntaş Bayır Z. Synthesis of quaternized zinc(II) and cobalt(II) phthalocyanines bearing pyridine-2-yl-ethynyl groups and their DNA binding properties. Turkish Journal of Chemistry 2018; 42: 572-585. https://doi.org/10.3906/kim-1707-54

[41] Koçan H, Kaya K, Özçeşmeci İ, Sesalan BŞ, Göksel M et al. Photophysicochemical, calf thymus DNA binding and in vitro photocytotoxicity properties of tetra-morpholinoethoxy-substituted phthalocyanines and their water-soluble quaternized derivatives. Journal of Biological Inorganic Chemistry 2017; 22: 1251-1266. https://doi.org/10.1007/s00775-017-1499-3

[42] Özçeşmeci M, Ecevit ÖB, Sürgün S, Hamuryudan E. Tetracationic fluorinated zinc(ii)phthalocyanine: Synthesis, characterization and DNA-binding properties. Dyes and Pigments 2013; 96: 52-58. https://doi.org/10.1016/j.dyepig.2012.06.018

[43] Lo PC, Zhao B, Duan W, Fong WP, Ko WH et al. Synthesis and in vitro photodynamic activity of mono-substituted amphiphilic zinc(II) phthalocyanines. Bioorganic & Medicinal Chemistry Letters 2007; 17 (4): 1073-1077. https://doi.org/10.1016/j.bmcl.2006.11.017

[44] Özçeşmeci M. Synthesis, photophysical and photochemical properties of metal-free and zinc(II) phthalocyanines bearing α-naphtholbenzein units. Journal of Organometallic Chemistry 2014; 767: 16-21. https://doi.org/10.1016/j.jorganchem.2014.05.015

[45] Karanlık CC, Atmaca GY, Erdoğmuş A. Comparison of singlet oxygen production of ethyl vanillin substituted silicon phthalocyanine using sonophotodynamic and photodynamic methods. Journal of Molecular Structure 2023; 1274: 134498. https://doi.org/10.1016/j.molstruc.2022.134498

[46] Keskin B, Okuyucu O, Altındal A, Erdoğmuş A. Novel indium(III) phthalocyanines; synthesis, photophysical and humidity sensing properties. New Journal of Chemistry 2016; 40: 5537-5545. https://doi.org/10.1039/c6nj00057f

[47] Atmaca GY, Karanlık CC, Erdoğmuş A. Novel silicon phthalocyanines with improved singlet oxygen generation by Sono-photochemical applications. Journal of Photochemistry and Photobiology, A: Chemistry 2023; 436: 114365. https://doi.org/10.1016/j.jphotochem.2022.114365

[48] Granados-Tavera K, Zambrano-Angulo M, Montenegro-Pohlhammer N, Atmaca GY, Sobotta L et al. Synergistic effect of ultrasound and light to efficient singlet oxygen formation for photodynamic purposes. Dyes and Pigments 2023; 210: 110986. https://doi.org/10.1016/j.dyepig.2022.110986

[49] Karanlık CC, Karanlık G, Taslimi P, Erdoğmuş A. Improvement of photochemical and enzyme inhibition properties of new BODIPY compound by conjugation with cisplatin. Polyhedron 2022; 225: 116042. https://doi.org/10.1016/j.poly.2022.116042

[50] Karanlık CC, Karanlık G, Erdoğmuş A. Water-soluble *meso*-thienyl BODIPY therapeutics: Synthesis, characterization, exploring photophysicochemical and DNA/BSA binding properties. Journal of Photochemistry and Photobiology, A: Chemistry 2023; 438: 114581. https://doi.org/10.1016/j.jphotochem.2023.114581

[51] Teng KX, Chen WK, Niu LY, Fang WH, Cui G et al. BODIPY-based photodynamic agents for exclusively generating superoxide radical over singlet oxygen. Angewandte Chemie International Edition 2021; 60: 19912-19920. https://doi.org/10.1002/anie.202106748

[52] Günsel A, Güzel E, Bilgiçli AT, Atmaca GY, Erdoğmuş A et al. Synthesis and investigation of photophysicochemical properties of novel ketone-substituted gallium (III) and indium (III) phthalocyanines with high singlet oxygen yield for photodynamic therapy. Journal of Luminescence 2017; 192: 888-892. https://doi.org/10.1016/j.jlumin.2017.08.014

[53] Köksoy MA, Köksoy B, Durmuş M, Bulut M. Preparation, characterization and photophysicochemical properties of novel tetra 7-(diethyl 2-methylmalonatoxy)-3-(*p*-oxyphenyl)coumarin-substituted zinc(II) and indium(III)chloride phthalocyanines. Journal of Organometallic Chemistry 2016; 822: 125-134. https://doi.org/10.1016/j.jorganchem.2016.08.009

[54] Nene LC, Nyokong T. The in-vitro proliferation-suppression of MCF-7 and HeLa cell lines mediated by differently substituted ionic phthalocyanines in sonodynamic therapy supplemented-photodynamic therapy. Journal of Inorganic Biochemistry 2023; 239: 112084. https://doi.org/10.1016/j.jinorgbio.2022.112084

[55] Atmaca GY, Aksel M, Bilgin MD, Erdoğmuş A. Comparison of sonodynamic, photodynamic and sonophotodynamic therapy activity of fluorinated pyridine substituted silicon phthalocyanines on PC3 prostate cancer cell line. Photodiagnosis and Photodynamic Therapy 2023; 42: 103339. https://doi.org/10.1016/j.pdpdt.2023.103339

[56] Can Karanlık C, Aguilar-Galindo F, Sobotta L, Güzel E, Erdoğmuş A. Combination of light and ultrasound: Exploring sono-photochemical activities of phthalocyanine-based sensitizers. The Journal of Physical Chemistry C, 2023; 127 (19): 9145-9153. https://doi.org/10.1021/acs.jpcc.3c01176

[57] Ünlü S, Elmalı FT, Atmaca GY, Erdoğmuş A. Synthesis of axially Schiff base new substituted silicon phthalocyanines and investigation of photochemical and sono-photochemical properties. Photodiagnosis and Photodynamic Therapy, 2022; 40: 103192. https://doi.org/10.1016/j.pdpdt.2022.103192

[58] Nene LC, Nyokong T. Enhancement of the in vitro anticancer photo-sonodynamic combination therapyactivity of cationic thiazole-phthalocyanines using gold and silver nanoparticles. Journal of Photochemistry and Photobiology A: Chemistry 2023; 435: 114339. https://doi.org/10.1016/j.jphotochem.2022.114339

[59] Durmuş M, Nyokong T. Synthesis, photophysical and photochemical properties of aryloxy tetra-substituted gallium and indium phthalocyanine derivatives. Tetrahedron 2007; 63: 1385-1394. https://doi.org/10.1016/j.tet.2006.11.089

Supplementary Information

Comparative sonophotochemical and photochemical studies of phthalocyanines with cationic substituents on non-peripheral positions

1. Materials and equipment

All reagents and solvents were of reagent grade quality and were obtained from commercial suppliers. ^{1}H NMR spectra of the synthesized compounds were recorded on an Agilent VNMRS 500 MHz spectrometer. FT-IR spectra were recorded on a PerkinElmer Spectrum One FT-IR spectrometer with a UATR (universal attenuated total reflectance sampling accessory) module. Electronic spectra were recorded on a Scinco SD 1000 diode array, single-beam ultraviolet–visible (UV–Vis) spectrophotometer. Mass spectra were performed on Bruker Microflex MALDI-TOF mass spectrometer. 3-[1,3-bis(dimethylamino)-2-propoxy]-1,2-dicyanobenzene (**1**), 1,8(11),15(18),22(25)-tetrakis(1,3-bis-(dimethylamino)-2-propoxy)phthalocyaninato zinc(II) (**3**) and [1,8(11),15(18),22(25)-tetrakis(1,3-bis-(trimethylamino)-2-propoxy) phthalo-cyaninatozinc(II)]octaiodide (**6**) were prepared according to the reported procedures [S1,S2].

Fluorescence spectra were measured using a Varian Eclipse spectrofluorometer using 1 cm path length cuvettes at room temperature. Photoirradiations were measured using a General Electric quartz line lamp (75W). A 600 nm glass cut off filter (Schott) and a water filter were used to filter off ultraviolet and infrared radiations respectively. Light intensities were measured with a POWER MAX5100 (Mol electron detector incorporated) power meter. Bandelin Ultrasonic RK 100 H was used for ultrasound irradiation.

2. Experimental

2.1. Synthesis

2.1.1. 1,8(11),15(18),22(25)-Tetrakis(1,3-bis-(dimethylamino)-2-propoxy) phthalocyanine (2)

0.010 g (1.5 mmol) of lithium metal in small amounts was mixed with 5 mL of n-pentanol and the mixture was stirred at 80 °C for 10 min. Compound **1** was added to the reaction mixture in the amount of 0.200 g (0.734 mmol), and the reaction temperature was raised to 145 °C. For an additional 5 h, the mixture was continued to be stirred in a closed tube under nitrogen atmosphere. The resulting green product was precipitated with cold water after cooling to room temperature. The metal-free phthalocyanine structure was obtained by protonation by adding 1 mL of glacial acetic acid. The product was purified using alumina-packed column chromatography and a THF/methanol (1:9) mixture as the eluent. $C_{60}H_{82}N_{16}O_4$; Yield: 0.074 g (37%). m.p. > 200°C. FT-IR ν/cm^{-1}: 3291 (N-H), 3068 (Ar-H), 2941–2770 (Aliph. C-H) 1584, 1485, 1258, 1019, 746. ^{1}H-NMR (DMSO-d_6, 500 MHz): 8.28–7.40 (m, 12H, Ar-H), 5.30 (br, 4H, OCH), 3.81 (m, 16H, NCH_2), 3.11 (s, 48H, NCH_3), –1.38 (br, 2H, NH) ppm. UV-Vis (THF), l_{max} (log ε): 319 (4.82), 694 (5.20), 726 (5.19) nm. MS (MALDI-TOF), (*m/z*) calcd. 1091.420 $[M]^+$; found: 1091.192 $[M]^+$

2.1.2. 1,8(11),15(18),22(25)-Tetrakis(1,3-bis-(dimethylamino)-2-propoxy) phthalocyaninatoindium(III)chloride (4)

0.050 g compound **2** (0.046 mmol) and 0.020 g $InCl_3$ (0.092 mmol) were mixed in a closed tube in 2-dimethylaminoethanol (2 mL) and stirred under a nitrogen atmosphere for 20 h at 140 °C. The product was cooled to room temperature and washed with water and methanol. After that, it was purified by alumina packed-column chromatography using a THF/methanol (1:9) mixture as the eluent. $C_{60}H_{80}ClInN_{16}O_4$; Yield: 0.020 g (35%). m.p. > 200 °C. FT-IR ν/cm^{-1}: 2942–2768 (Aliph. C-H), 1607, 1393, 1224, 1089, 829, 702. ^{1}H-NMR (DMSO-d_6, 500 MHz): 9.22–7.78 (m, 12H, Ar-H), 5.12 (m, 4H, OCH), 2.83 (m, 16H, NCH_2), 2.42 (s, 48H, NCH_3) ppm. UV-Vis (THF), l_{max} (log ε): 322 (5.31), 717 (4.95) nm. MS (MALDI-TOF), (*m/z*) calcd. 1239.68 $[M]^+$; found: 1239.159 $[M]^+$.

2.1.3. [1,8(11),15(18),22(25)-Tetrakis[1,3-bis-(trimethylamino)2-propoxy) phthalocyanine]octaiodide (5)

0.050 g compound **2** (0.046 mmol) and 0.653 g methyl iodide (0.460 mmol) were refluxed in 30 mL of chloroform for 20 h. Then the reaction solvent was removed under vacuum. The resulting product was washed repeatedly using chloroform, dichloromethane, methanol, ethanol, and ethyl acetate solvents. $C_{68}H_{106}I_8N_{16}O_4$; Yield: 0.063 g (62%). m.p. > 200 °C. FT-IR ν/cm^{-1}: 3291 (N-H), 3011 (Ar-H), 2941-2831 (Aliph. C-H), 1473, 1214, 1094, 973, 746. ^{1}H NMR (DMSO-d_6, 500 MHz): 9.11–7.49 (br, 12H, Ar-H), 6.27 (br, 4H, OCH), 4.63 (br, 16H, NCH_2), 3.09 (s, 72H, NCH_3), –1.40 (br, 2H, NH) ppm. UV-Vis (DMSO), l_{max} (log ε): 322 (4.27), 693 (4.55) nm. UV-Vis (H_2O), l_{max} (log ε): 319 (4.19), 693 (4.44) nm. MS (MALDI-TOF), (*m/z*) calcd. 2226.940 $[M]^+$, found: 1338.573 $[M - 7I]^+$, 1211.111 $[M - 8I]^+$.

2.1.4. *[1,8(11),15(18),22(25)-Tetrakis[1,3-bis-(trimethylamino)2-propoxy) phthalocyaninatoindium(III)chloride] octaiodide (7)*

Compound **7** was synthesized according to the procedure described for **5**. The amounts of reactants used in this synthesis were as follows: Compound **4** (0.037 g, 0.030 mmol), methyl iodide (0.043 g, 0.303 mmol) in chloroform (30 mL).

$C_{68}H_{104}I_8ClInN_{16}O_4$; Yield: 0.029 g (41%). m.p. > 200 °C. FT-IR ν/cm^{-1}: 3009 (Ar-H), 2953-2857 (Aliph. C-H), 1477, 1231, 1124, 1049, 926, 745. ^{1}H NMR (DMSO-d_6, 500 MHz): 9.41–8.17 (br, 12H, Ar-H), 6.16 (br, 4H, OCH), 4.19 (br, 16H, NCH_2), 3.43 (s, 72H, NCH_3) ppm. UV-Vis (DMSO), l_{max} (log ε): 327 (4.31), 720 (4.47) nm; UV-Vis (H_2O), l_{max} (log ε): 335 (4.47), 715 (4.44) nm. MS (MALDI-TOF), (*m/z*) calcd. 2375.190 $[M]^+$, found: 1740.699 $[M - 5I]^+$, 1360.171 $[M - 8I]^+$.

3. Photophysical and photochemical studies

3.1. Fluorescence quantum yields (Φ_F)

Fluorescence quantum yield (Φ_F) was determined by applying the comparative method (Eq. 1) [S3],

$$\Phi_F = \Phi_{F(Std)} \frac{F \cdot A_{Std} \cdot n^2}{F_{Std} \cdot A \cdot n^2_{Std}} \quad (1)$$

where F and F_{Std} are the area under the fluorescence emission curves of the sample and the standard, respectively. A and A_{Std} are the respective absorbances of the samples and standard (Unsubstituted **ZnPc**) at the excitation wavelengths, respectively. n^2 and n^2_{Std} are the refractive indices of solvents used for the sample and standard, respectively. Unsubstituted **ZnPc** (Φ_F = 0.20 in DMSO) [S3] was used as the standard. Both the samples and standards were excited at the same wavelength.

3.2. Singlet oxygen quantum yields (Φ_Δ)

Singlet oxygen efficiency was determined in the air (no oxygen bubbled) using the relative method (Eq. 2) with unsubstituted ZnPc as reference and 1,3-diphenylisobenzofuran (DPBF) as chemical quencher for singlet oxygen,

$$\Phi_\Delta = \Phi_\Delta^{Std} \frac{R \cdot I_{abs}^{Std}}{R^{Std} \cdot I_{abs}} \quad (2)$$

where Φ_Δ^{Std} is the singlet oxygen quantum yield for the standard ZnPc (Φ_Δ^{Std} = 0.67 in DMSO) [S2]. R and R_{Std} are the DPBF photobleaching rates in the presence of the respective samples and standard, respectively. I_{abs} and are the rates of light absorption by the sample and standard, respectively. The samples containing DPBF were prepared in the dark and irradiated at the Q band region. The absorption band of the DPBF was reduced by light irradiation (The light intensity of 7.05×10^{15} photons s^{-1} cm^{-2}). The degradation of DPBF was monitored using UV-Vis spectroscopy after each 5 s light irradiation at about 417 nm for photochemical studies. For sonophotochemical studies, the sample (the compound+DPBF) was monitored after each 10 s irradiation (5 s by light intensity of 7.05×10^{15} photons s^{-1} cm^{-2} and 5 s by ultrasound at a frequency of 35 kHz).

3.3. Photodegradation quantum yields (Φ_d)

Photodegradation quantum yields were determined using Eq. 3,

$$\Phi_d = \frac{(C_0 - C_t) \cdot V \cdot N_A}{I_{abs} \cdot S \cdot t} \quad (3)$$

where "C_0" and "C_t" are the sample concentrations before and after irradiation respectively, "V" is the reaction volume, "N_A" is the Avogadro's constant, "S" is the irradiated cell area, "t" is the irradiation time, "I_{abs}" is the overlap integral of the radiation source light intensity and the absorption of the sample. A light intensity of 2.42×10^{16} photons s^{-1} cm^{-2} and/or ultrasound at a frequency of 35 kHz was employed to determine photodegradation [S3,S4]. The degradation of max. Q band was monitored after each 10-min irradiation.

References

[S1] Lo PC, Zhao B, Duan W, Fong WP, Ko WH et al. Synthesis and in vitro photodynamic activity of mono-substituted amphiphilic zinc(II) phthalocyanines. Bioorganic & Medicinal Chemistry Letters 2007; 17 (4): 1073-1077. https://doi.org/10.1016/j.bmcl.2006.11.017

[S2] Özçeşmeci M, Sancar Baş S, Akkurt B, Bolkent Ş, Hamuryudan E. Synthesis, characterization and staining performance of peripherally and non-peripherally substituted metallo-phthalocyanines bearing 1,3-bis-(trimethylamino)-2-propoxy groups. New Journal of Chemistry 2020; 44: 7786-7794. doi: 10.1039/d0nj01404d

[S3] Tayfuroğlu O, Atmaca GY, Erdoğmuş A. Novel peripherally substituted zinc phthalocyanine: synthesis, characterization, investigation of photophysicochemical properties and theoretical study. Journal of Coordination Chemistry. 2017; 70: 3095-3109. doi: 10.1080/00958972.2017.1377340

[S4] Tayfuroğlu O, Kılıçarslan FA, Atmaca GY, Erdoğmuş A. Synthesis, characterization of new phthalocyanines and investigation of photophysical, photochemical properties and theoretical studies. Journal of Porphyrins and Phthalocyanines 2018; 22: 250-265. doi: 10.1142/S1088424618500281

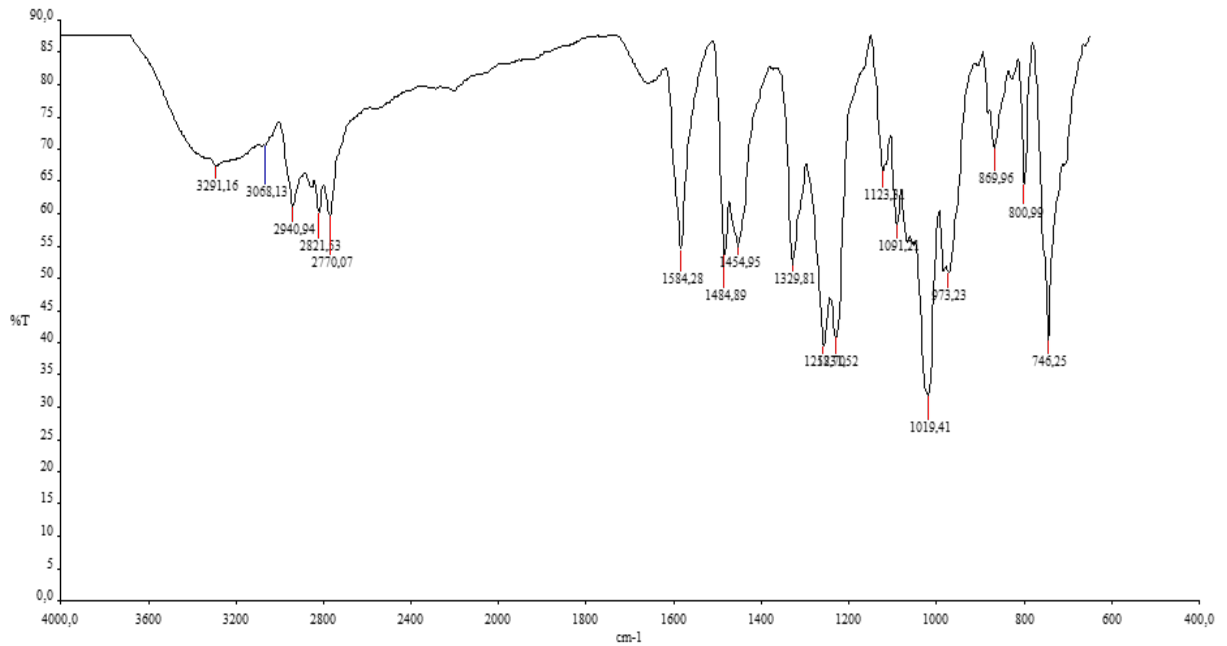


Figure S1. FT-IR spectrum of **2**.

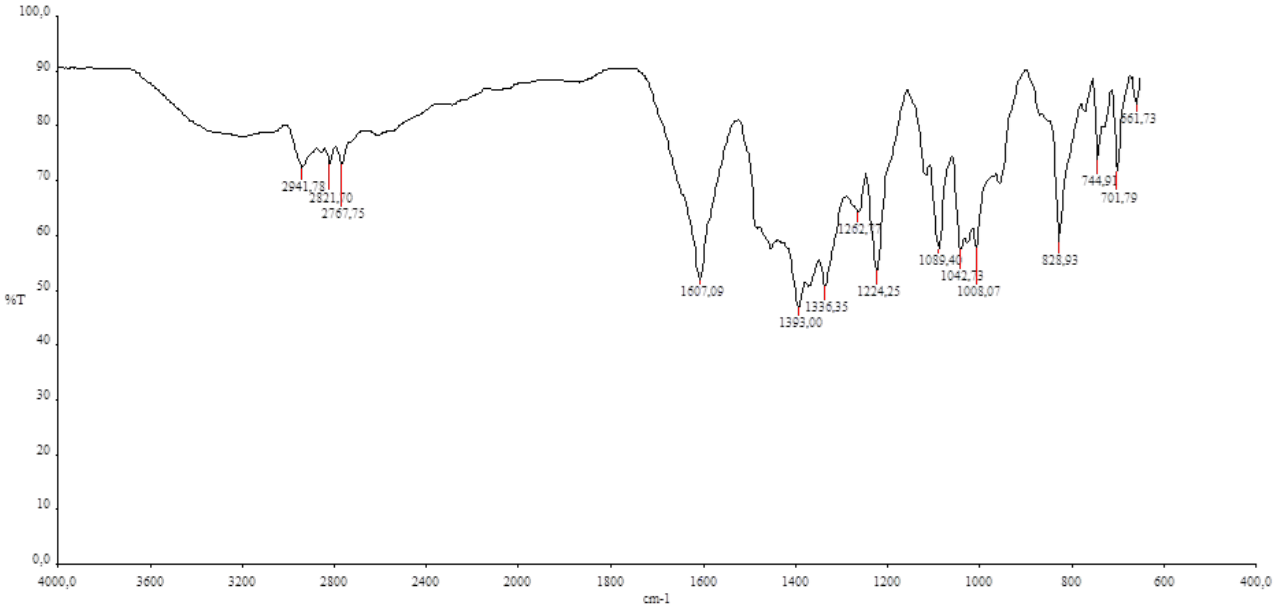


Figure S2. FT-IR spectrum of **4**.

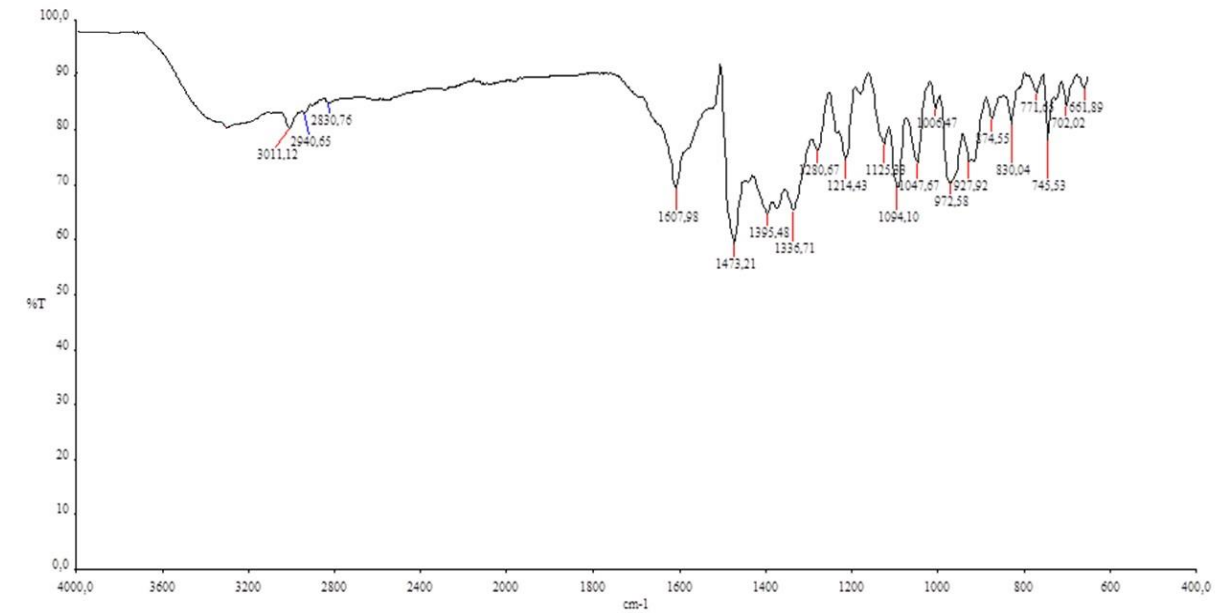


Figure S3. FT-IR spectrum of **5**.

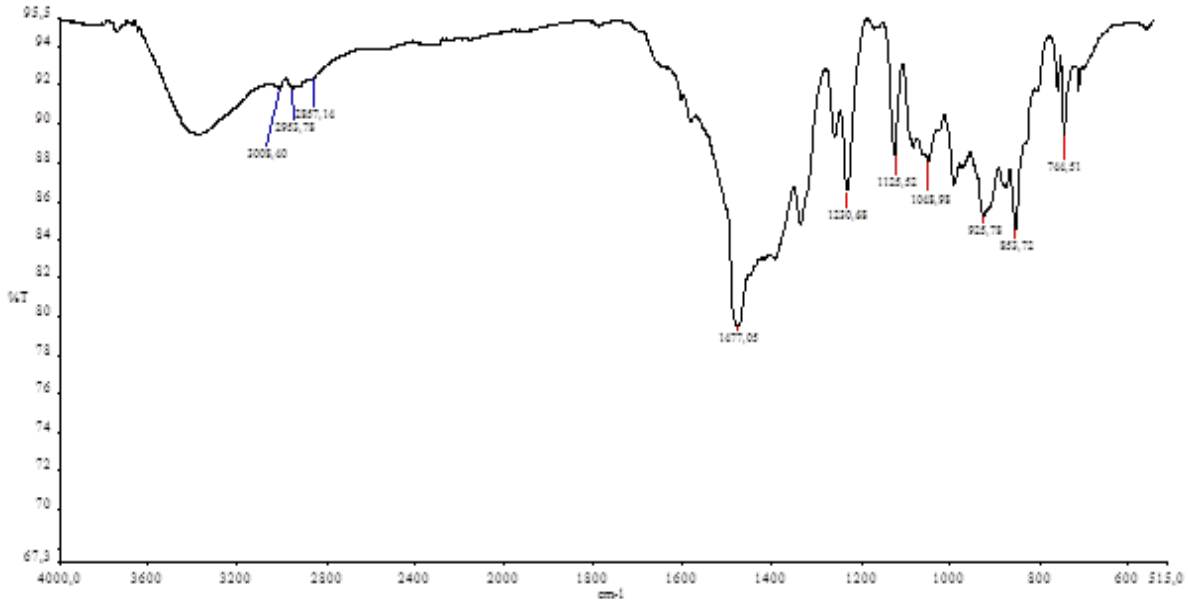


Figure S4. FT-IR spectrum of **7**.

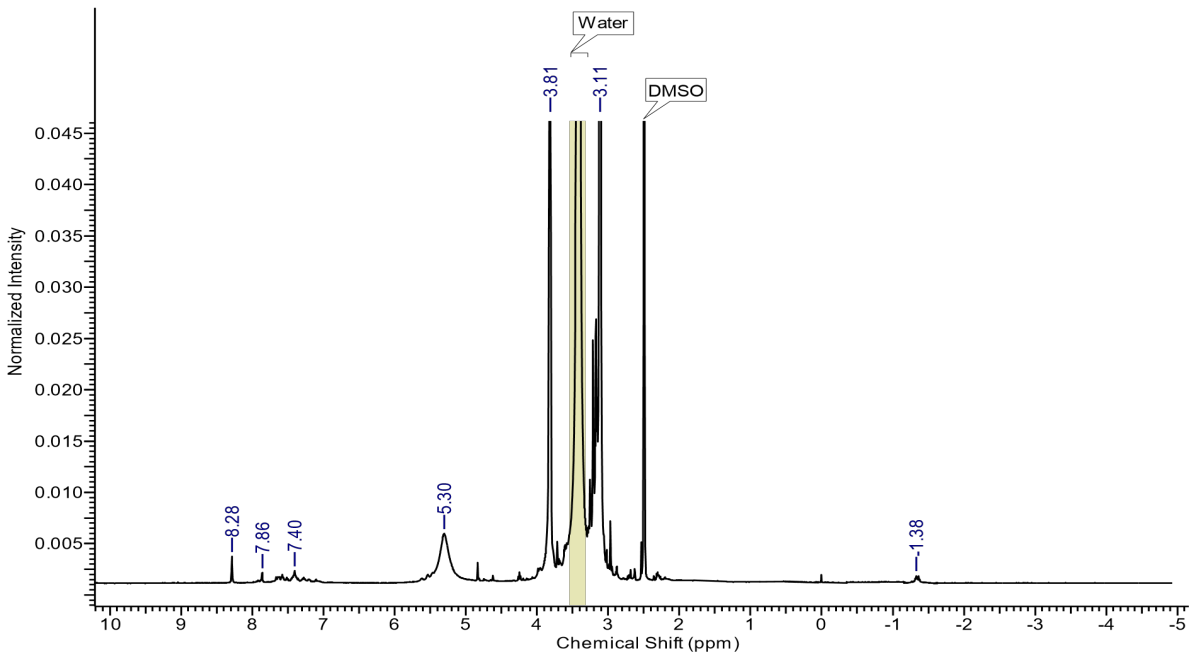


Figure S5. ^{1}H NMR spectrum of **2** in d_6-DMSO.

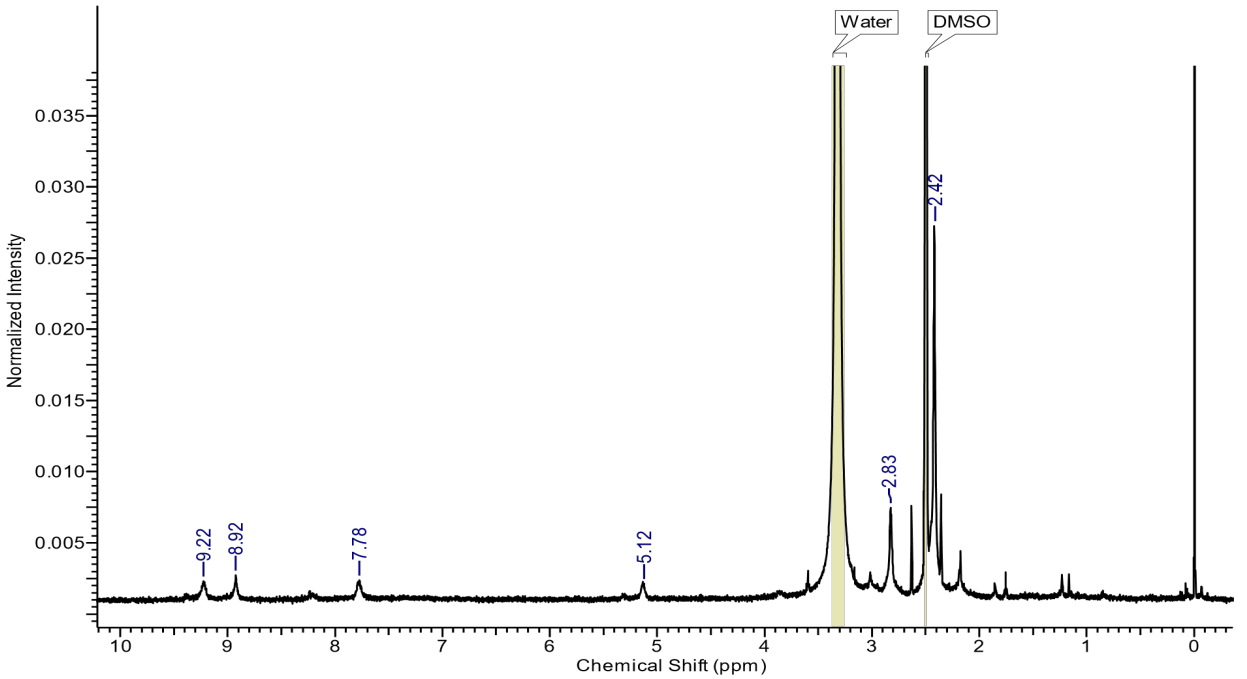


Figure S6. ^{1}H NMR spectrum of **4** in d_6-DMSO.

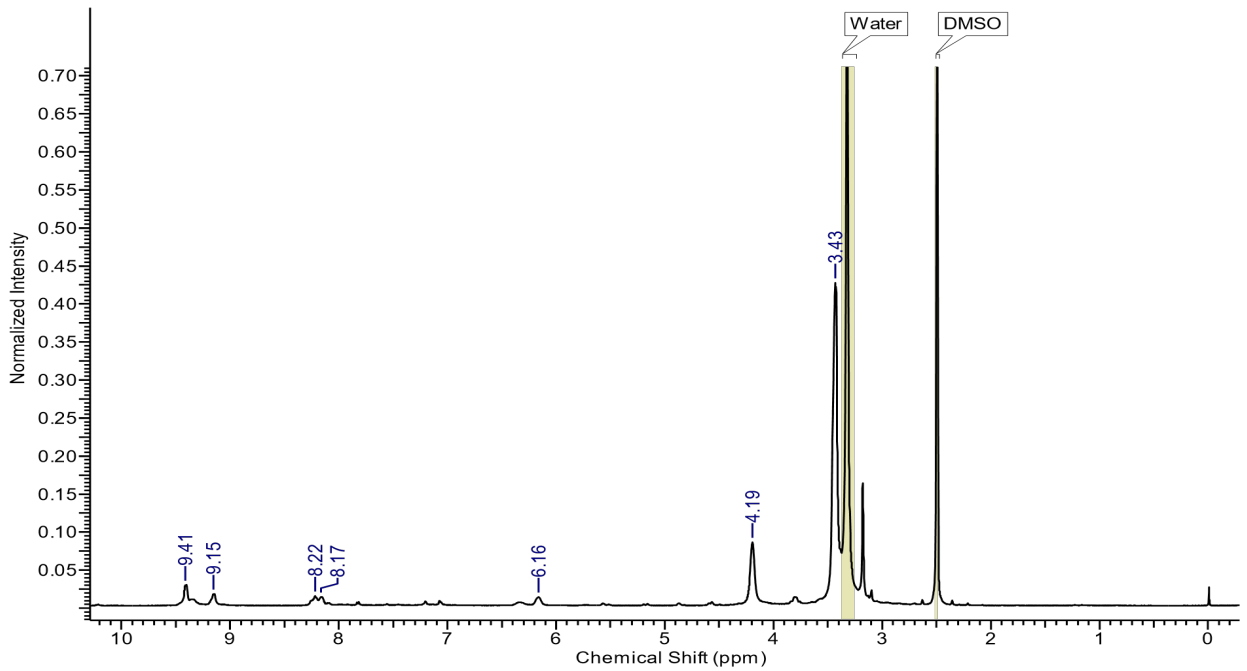


Figure S7. ^{1}H NMR spectrum of **7** in d_6-DMSO.

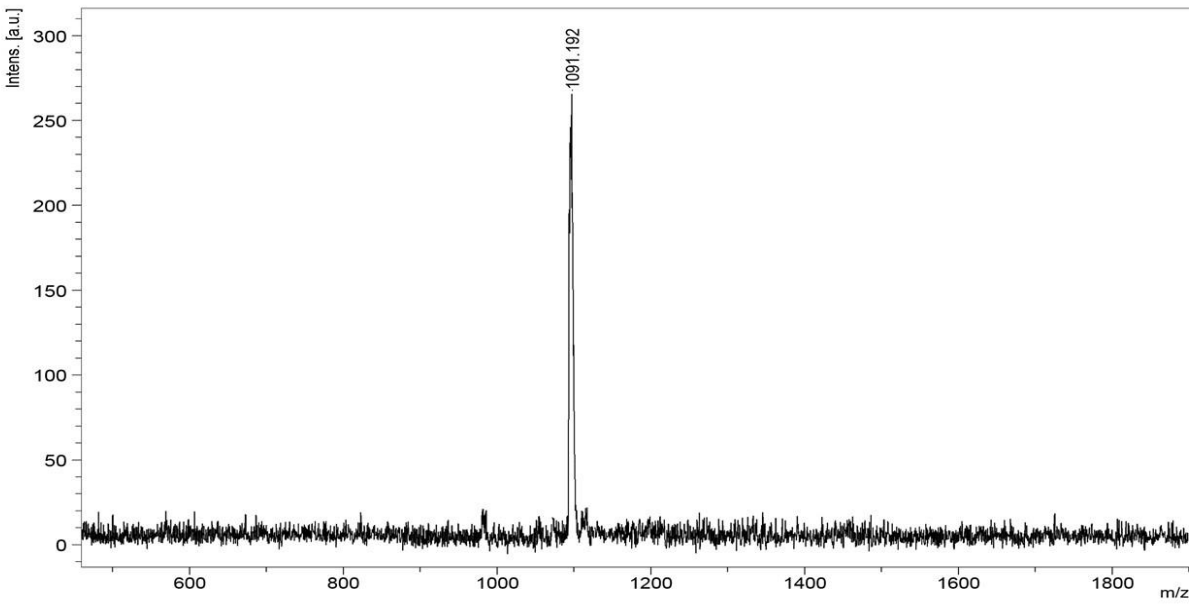


Figure S8. MALDI-TOF MS spectrum of **2**.

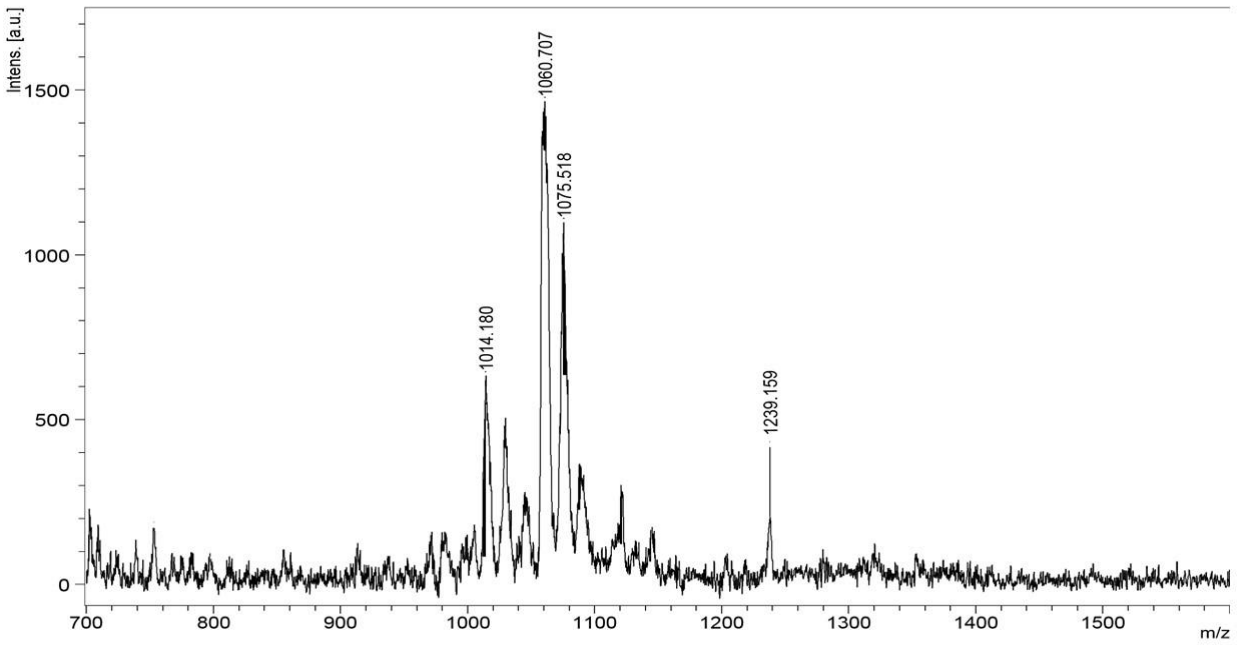


Figure S9. MALDI-TOF MS spectrum of **4**.

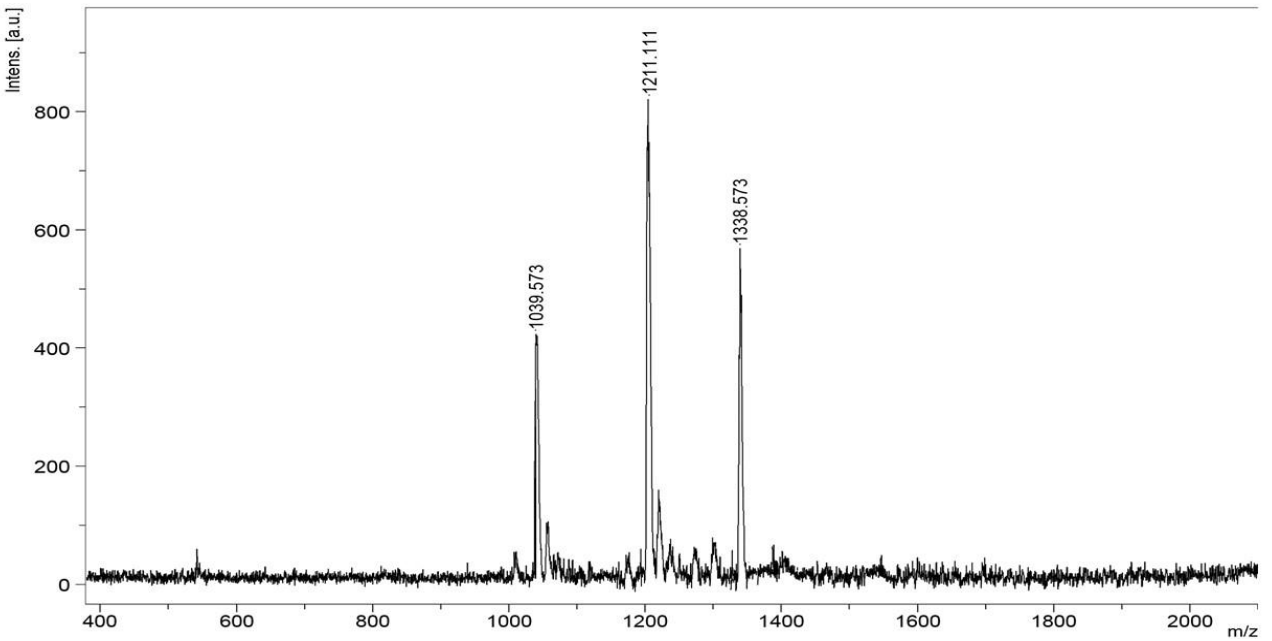


Figure S10. MALDI-TOF MS spectrum of **5**.

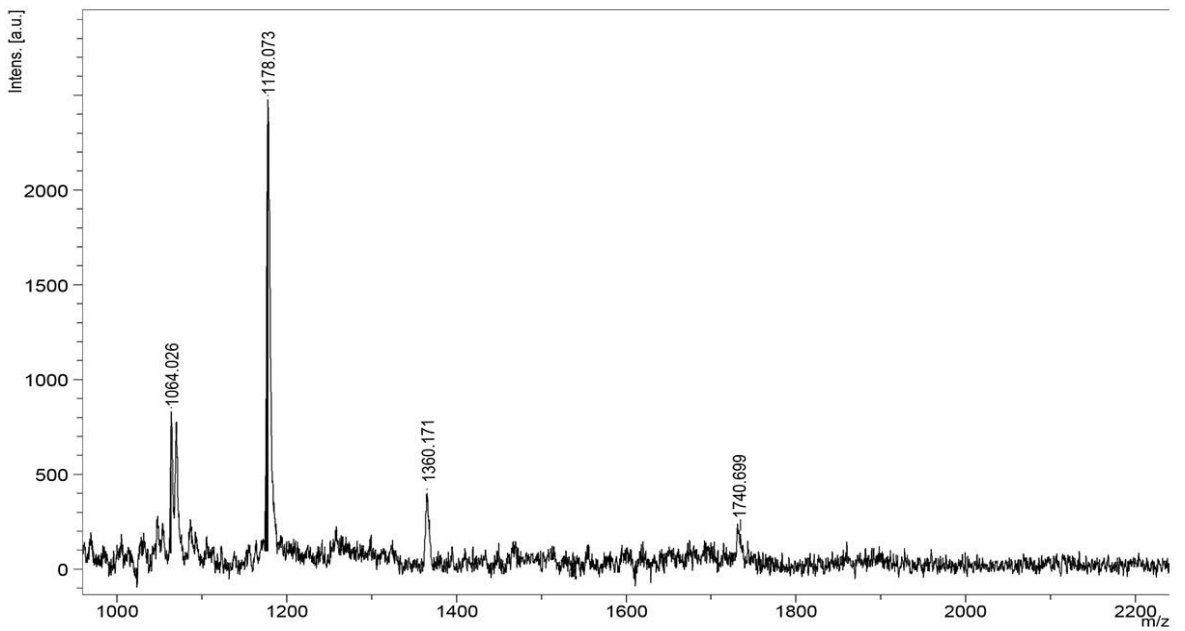


Figure S11. MALDI-TOF MS spectrum of **7**.